Internal Medicine
The Japanese Society of Internal Medicine
doi: 10.2169/internalmedicine.3023-23
Intern Med 63: 2325-2329, 2024
http://internmed.jp

【 CASE REPORT 】

^{18}F-THK5351 Positron Emission Tomography Clearly Depicted Progressive Multifocal Leukoencephalopathy after Mantle Cell Lymphoma Treatment

Yuta Chiba[1], Rie Kawakita[1], Katsuya Mitamura[2], Kenta Takahashi[3], Tadaki Suzuki[3], Kazuo Nakamichi[4], Kenta Suzuki[5], Asahiro Morishita[1], Hideki Kobara[1], Kazushi Deguchi[1] and Tsutomu Masaki[1]

Abstract:

An 84-year-old Japanese woman presented with left hemiplegia 8 months after completing chemotherapy for mantle cell lymphoma. Brain magnetic resonance imaging (MRI) revealed a hyperintense lesion extending from the right parietal lobe to the left parietal lobe. Compared with these MRI results, ^{18}F-THK5351 PET revealed more extensive accumulation. A brain biopsy showed progressive multifocal leukoencephalopathy (PML). Immunohistochemistry and John Cunningham virus (JCV) DNA-polymerase chain reaction indicated JCV infection. Therefore, a diagnosis of PML was made. ^{18}F-THK5351 PET, indicative of activated astrocytes, clearly depicted PML lesions composed of reactive and atypical astrocytes. ^{18}F-THK5351 PET may capture fresh progressive PML lesions better than MRI.

Key words: ^{18}F-THK5351 PET, progressive multifocal leukoencephalopathy, lymphoma, astrocyte, monoamine oxidase B, JC virus

(Intern Med 63: 2325-2329, 2024)
(DOI: 10.2169/internalmedicine.3023-23)

Introduction

Mantle cell lymphoma (MCL) is a B-cell tumor that accounts for 5-7% of non-Hodgkin lymphomas (1). If central nervous system (CNS) involvement occurs after a patient is treated for MCL, the potential development of progressive multifocal leukoencephalopathy (PML) and brain recurrence of MCL should be considered, as both the lymphoma itself and the drugs used to treat MCL are risk factors for the development of PML (2). Although histologic findings are necessary to differentiate between MCL and PML, positron emission tomography (PET) findings reflecting lesion characteristics might help achieve the diagnosis.

We herein report a patient with rapidly progressing CNS involvement observed under conditions of persistent lymphopenia eight months after the completion of bendamustine + rituximab combination (BR) therapy and rituximab maintenance therapy for MCL. ^{18}F-THK5351 PET showed the marked accumulation of ^{18}F-THK5351, which was consistent with the appearance of pathologically confirmed reactive and atypical astrocytes (including bizarre astrocytes). This report is the first to confirm that the accumulation of ^{18}F-THK5351 on PET enables the identification of critical lesions in PML.

Case Report

An 84-year-old Japanese woman developed MCL and was treated for 6 months with BR therapy, followed by 21

[1]Department of Gastroenterology and Neurology, Graduate School of Medicine and Faculty of Medicine, Kagawa University, Japan, [2]Department of Radiology, Graduate School of Medicine and Faculty of Medicine, Kagawa University, Japan, [3]Department of Pathology, National Institute of Infectious Diseases, Japan, [4]Department of Virology 1, National Institute of Infectious Diseases, Japan and [5]Department of Neurosurgery, Graduate School of Medicine and Faculty of Medicine, Kagawa University, Japan
Received: October 6, 2023; Accepted: November 15, 2023; Advance Publication by J-STAGE: January 2, 2024
Correspondence to Dr. Kazushi Deguchi, deguchi.kazushi@kagawa-u.ac.jp

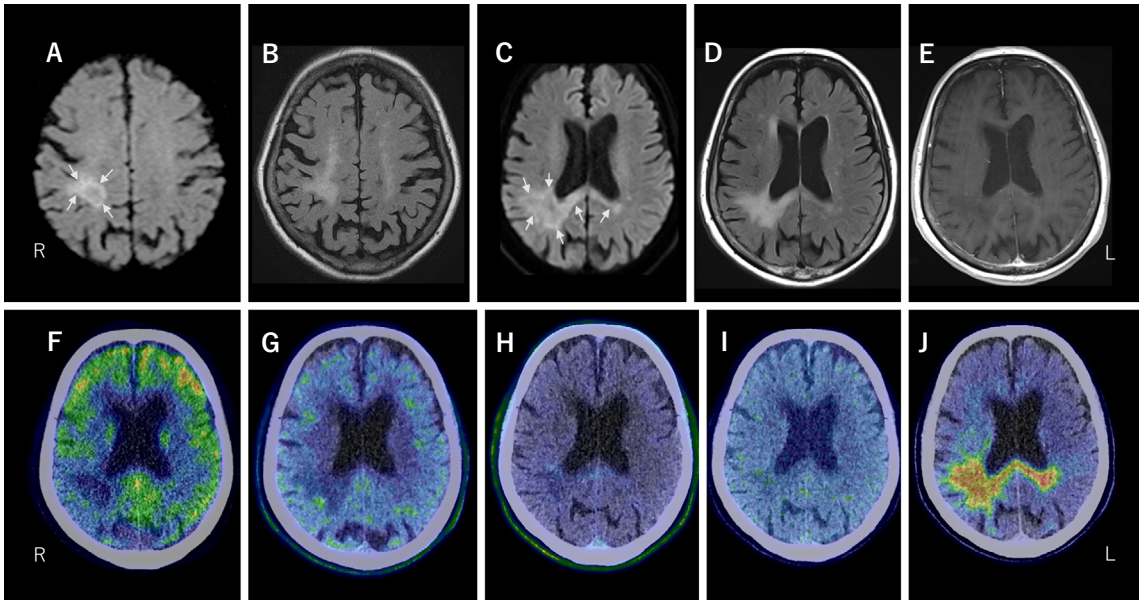

Figure 1. **Brain MRI on day 4 (A, B) and 44 (C-E) after the onset. A, C: DWI showed intense hyperintensity at the edges of the lesion (*arrows*). B, D: FLAIR images revealed hyperintensity throughout the lesion. The lesion at the onset was confined to the upper right parietal lobe (A, B) and thereafter descended from the upper right parietal lobe and extended through the corpus callosum to the left parietal lobe (C, D). E: Gadolinium enhancement on T1-weighted imaging was not observed. PET imaging with ^{18}F-fluorodeoxyglucose (FDG) (F), ^{11}C-methionine (MET) (G), ^{18}F-fluoro-3´-deoxy-3´-L-fluorothymidine (FLT) (H), ^{18}F-fluoromisonidazole (FMISO) (I), and ^{18}F-THK5351 (J). Of these, only ^{18}F-THK5351-PET demonstrated a marked accumulation of ^{18}F-THK5351 consistent with the lesion on MRI. Panels F-J are merged PET and CT images.**

months of rituximab maintenance therapy. Eight months after completing the treatment, she developed mild weakness in the left upper and lower extremities [Medical Research Council (MRC) scores, 4/5]. Brain magnetic resonance imaging (MRI) revealed hyperintensity confined to the right parietal lobe on diffusion-weighted imaging (DWI) and fluid-attenuated inversion recovery (FLAIR) images (Fig. 1).

Despite treatment based on a diagnosis of cerebral infarction, the patient's left-sided weakness progressively worsened, and the lesion was observed on MRI. On day 40, the patient was transferred to our hospital. Her body temperature was 36.7°C, blood pressure was 115/67 mmHg, and pulse rate was 72 beats/min. She was awake and alert. Left facial paralysis, mild dysarthria, and tongue deviation to the left side were observed. The left upper and lower extremities were completely paralyzed. The tendon reflexes were exaggerated in the left upper and lower extremities, and the left plantar response was extended. Superficial sensory disturbances were observed on the left side of the body. Other than lymphopenia (511/μL) and a slightly elevated soluble interleukin-2 receptor level (716 U/mL), routine blood test results were unremarkable. The HIV antibody test results were negative.

Brain MRI on day 44 showed a lesion expanding acutely from the right to the left parietal lobe through the corpus callosum, which was hyperintense on FLAIR images and hypointense on T1-weighted imaging (T1-WI), showing no gadolinium enhancement on T1-WI. Hyperintensity on DWI was observed at the edges of the lesion (Fig. 1). A series of PET studies were performed between days 40 and 50. ^{18}F-fluorodeoxyglucose (FDG)-PET showed no abnormal accumulation of FDG in the parietal lobe lesion, whereas ^{11}C-methionine (MET)-PET showed subtle ^{11}C-MET accumulation in part of the lesion margin. ^{18}F-fluoro-3´-deoxy-3´-L-fluorothymidine (FLT)-PET showed a slight accumulation. ^{18}F-fluoromisonidazole (FMISO) showed no abnormal accumulation.

In contrast, ^{18}F-THK5351 PET demonstrated the marked accumulation of ^{18}F-THK5351, which was consistent with the lesion on MRI. The uptake of ^{18}F-THK5351 appeared to extend beyond the hyperintense lesions on FLAIR and beyond the hyperintense lesion edges on DWI (Fig. 1).

A biopsy of the lesion site with the highest ^{18}F-THK5351 uptake was performed on day 55. A triad of classic PML was observed: demyelination, oligodendroglia with enlarged hyperchromatic nuclei, and atypical astrocytes, including enlarged, bizarre astrocytes with irregularly lobulated nuclei. The immunohistochemistry results for John Cunningham virus (JCV) VP1, JCV VP2/3, and JCV agnoprotein were positive, indicating JCV infection (Fig. 2). JCV DNA polymerase chain reaction (PCR) revealed 6,880 copies/cell in the biopsy specimen and 802 copies/cell in the cerebrospinal fluid (CSF). CSF findings showed slightly elevated protein (60 mg/dL) with pleocytosis (mononuclear cells 13/μL, polynuclear cells <1/μL) and markedly increased total tau (T-tau) (1,320 pg/mL; normal range: 146-410 pg/mL) but

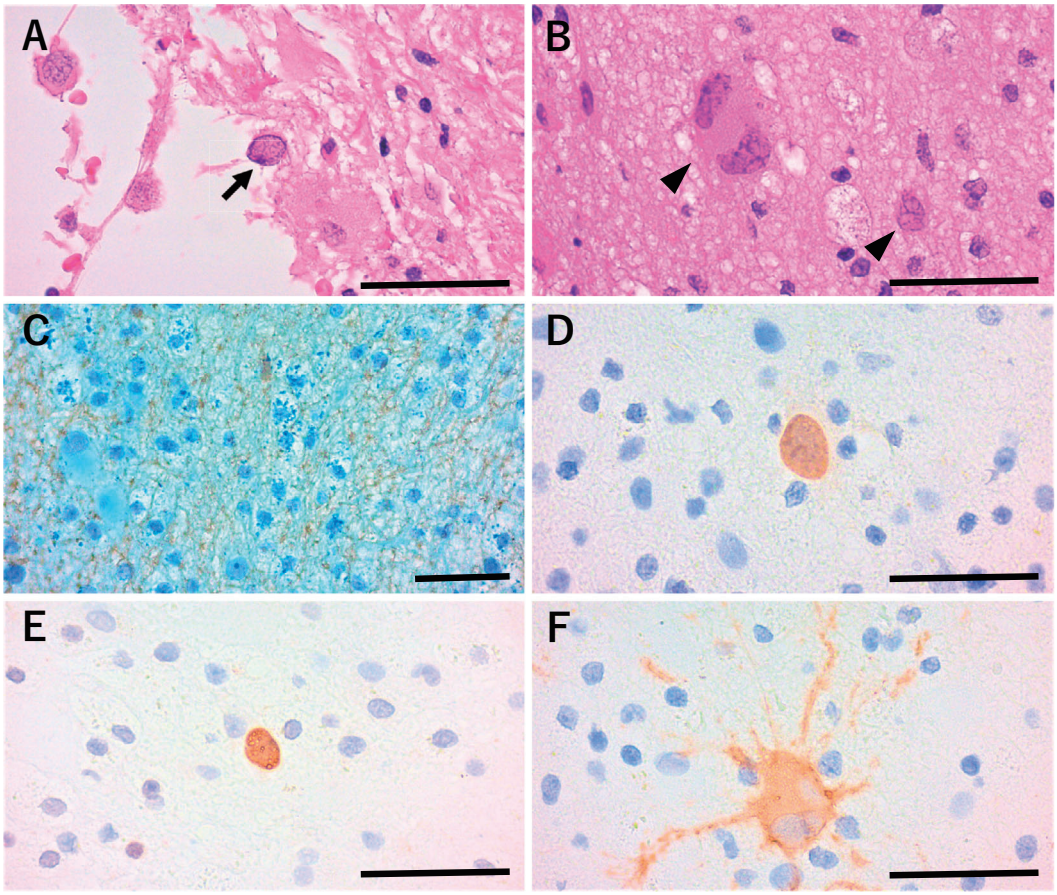

Figure 2. **Histopathology with the patient's brain biopsy. Oligodendroglia with enlarged hyperchromatic nuclei (*arrow*) (A) and atypical astrocytes (*arrowheads*), including bizarre astrocytes with irregularly lobulated nuclei, as well as reactive astrocytes and macrophage foam cells (B), were observed (Hematoxylin and Eosin staining). Demyelination (C) was observed (Klüver-Barrera stain and immunohistochemistry for neurofilament). Immunohistochemistry of JCV protein was positive for VP1 in the nuclei and cytoplasm (D), JCV VP2/3 in the nuclei (E), and JCV agnoprotein in the cytoplasm (F). Scale bars: 50 μm.**

not phosphorylated tau (P-tau) (39.2 pg/mL; normal range: 21.5-59.0 pg/mL). A diagnosis of definite PML was made based on the histopathological triad of the detection of JCV protein and JCV DNA (2).

On day 76, combination therapy (mefloquine and mirtazapine) was initiated, but the patient's neurological symptoms and MRI findings remained unchanged. On day 132, a JCV DNA PCR analysis of her CSF revealed 853 copies/cell. Lymphopenia (CD4+ T lymphocyte count, 120/μL) persisted. On day 147, the patient was transferred to another hospital for rehabilitation.

Discussion

PML is caused by the reactivation of JCV due to CD4+ T-cell deficiencies. The most striking risk factors for PML are particular underlying diseases, such as HIV infection, hematologic malignancy, natalizumab use, and other immunosuppressed states (2). An increasing number of drugs have been associated with the risk of PML (2). In our patient, prolonged and sustained CD4+ T-cell deficiency due to BR and rituximab maintenance therapy for MCL might have caused the onset of PML (3, 4).

The long-term use of drugs associated with PML risk and the edges of lesions with restricted diffusion on MRI (5) suggested PML in our patient rather than intra-CNS recurrence of MCL or glioblastoma. As a preliminary examination prior to a histological examination, PET might provide useful information to differentiate PML from other disorders. The FDG uptake in PML lesions is low, regardless of whether they are active or inactive, reflecting poor inflammatory cell infiltration into PML lesions and decreased glucose metabolism. Notably, PMLs with immune reconstruction inflammatory syndrome (IRIS) can have a high FDG uptake. Thus, FDG-PET does not appear to be a useful imaging modality for making a PML diagnosis (6). In contrast, ^{11}C-MET-PET shows an increased uptake around a PML lesion, reflecting protein synthesis during JCV replication and nuclear inclusion body formation in JCV-infected cells at the lesion margins (7). FLT-PET and 4′-[methyl-^{11}C] thiothymidine (4DST)-PET, which reflect the activation of DNA synthesis and cell proliferation as in malignancy, do not

show a clear uptake in PML (8).

The radiotracer ^{18}F-THK5351 binds to both tau aggregates and monoamine oxidase B (MAO-B) expressed on the outer mitochondrial membrane of astrocytes. In our patient, there was a marked increase in CSF T-tau without an increase in CSF P-tau, suggesting that severe neuronal damage not associated with tau formation occurred (9). As changes in MAO-B activity are an indicator of activated astrocytes, it is likely that the ^{18}F-THK5351 uptake reflects astrogliosis in disorders such as post-stroke Wallerian degeneration, multiple sclerosis, and PML (10). The ^{18}F-THK5351 uptake in our patient's case may therefore reflect astrogliosis rather than tau aggregates. However, the concordance between ^{18}F-THK5351 uptake and astrogliosis in these diseases has not been confirmed histologically. In our patient, tissue obtained from the site with the highest ^{18}F-THK5351 uptake clearly demonstrated the presence of reactive and atypical astrocytes, including bizarre astrocytes. This finding is the first evidence that ^{18}F-THK5351 does indeed reflect critical lesions in PML. However, primary lymphomas of the CNS do not appear to show a ^{18}F-THK5351 uptake (11). ^{18}F-THK 5351-PET might therefore be a useful imaging modality for differentiating PML from recurrent lymphoma, especially in conditions following the use of drugs associated with PML risk.

In the present patient, the ^{18}F-THK5351 uptake extended beyond the lesion, as detected by both DWI and FLAIR images. It is thought that restricted diffusion at the leading edges of expanding lesions results from the swelling of dying oligodendrocytes and astrocytes (5). Since JCV replication is observed primarily in astrocytes rather than oligodendrocytes (12), the outermost layer of the ^{18}F-THK5351 uptake extending beyond restricted diffusion might reflect the activated astrocytes associated with JCV replication. Thus, the ^{18}F-THK5351 uptake might better capture fresh lesions at the interface between PML lesions and normal tissue than MRI.

Several limitations associated with the present study warrant mention. First, some degree of reactive astrogliosis is expected in many CNS diseases, such as post-stroke Wallerian degeneration and multiple sclerosis (10); thus, the ^{18}F-THK5351 uptake is not specific to PML. Second, patient background factors (underlying disease, treatment history, and degree of IRIS) might influence the results of PET, including PET using FDG or ^{18}F-THK5351; for example, PML patients with IRIS can show a high FDG uptake (6). It should be noted that the differences in the FDG and ^{18}F-THK5351 uptake described herein were observed in a patient with long-lasting lymphopenia (without IRIS) after completing BR and rituximab maintenance therapy for MCL.

In conclusion, the gold standard for differentiating PML from recurrent lymphoma in patients treated for lymphoma is histopathological findings with the detection of JCV protein and JCV DNA. In our patient, the uptake region of ^{18}F-THK5351 demonstrated pathological findings of PML (i.e. reactive astrocytes and atypical astrocytes, including bizarre astrocytes). The abnormal accumulation of ^{18}F-THK5351 may indicate the probability of a PML diagnosis before a brain biopsy is conducted, and this might indicate that the border of JCV replication is now in progress in PML.

Informed consent was obtained from the patient's family for the clinical examination (including a series of PET studies) and for the publication of the patient's clinical and imaging data.

The authors state that they have no Conflict of Interest (COI).

Financial Support

This work was partially supported by the Research Committee of Prion Disease and Slow Virus Infection, Research on Policy Planning and Evaluation for Rare and Intractable Diseases, Health and Labor Sciences Research Grants from the Ministry of Health, Labor and Welfare of Japan (nos. 20FC0201 and 23FC 1007), and by JSPS KAKENHI (no. 21K07450).

Acknowledgement

We sincerely thank Prof. Hirofumi Sawa of Hokkaido University for providing antibodies to JCV proteins.

References

1. Armitage JO, Longo DL. Mantle-cell lymphoma. N Engl J Med **386**: 2495-2506, 2022.
2. Cortese I, Reich DS, Nath A. Progressive multifocal leukoencephalopathy and the spectrum of JC virus-related disease. Nat Rev Neurol **17**: 37-51, 2021.
3. Carson KR, Evens AM, Richey EA, et al. Progressive multifocal leukoencephalopathy after rituximab therapy in HIV-negative patients: a report of 57 cases from the Research on Adverse Drug Events and Reports project. Blood **113**: 4834-4840, 2009.
4. Martínez-Calle N, Hartley S, Ahearne M, et al. Kinetics of T-cell subset reconstitution following treatment with bendamustine and rituximab for low-grade lymphoproliferative disease: a population-based analysis. Br J Haematol **184**: 957-968, 2019.
5. Bergui M, Bradac GB, Oguz KK, et al. Progressive multifocal leukoencephalopathy: Diffusion-weighted imaging and pathological correlations. Neuroradiology **46**: 22-25, 2004.
6. Baldassari LE, Wattjes MP, Cortese ICM, et al. The neuroradiology of progressive multifocal leukoencephalopathy: a clinical trial perspective. Brain **145**: 426-440, 2022.
7. Shirai S, Yabe I, Kano T, et al. Usefulness of ^{11}C-methionine-positron emission tomography for the diagnosis of progressive multifocal leukoencephalopathy. J Neurol **261**: 2314-2318, 2014.
8. Ishibashi K, Miura Y, Matsumura K, et al. PET imaging of ^{18}F-FDG, ^{11}C-methionine, ^{11}C-flumazenil, and ^{11}C-4DST in progressive multifocal leukoencephalopathy. Intern Med **56**: 1219-1223, 2017.
9. Jack CR Jr, Bennett DA, Blennow K, et al. NIA-AA Research Framework: toward a biological definition of Alzheimer's disease. Alzheimers Dement **14**: 535-562, 2018.
10. Ishibashi K, Kameyama M, Miura Y, Toyohara J, Ishii K. Head-to-head comparison of the two MAO-B Radioligands, ^{18}F-THK5351 and ^{11}C-L-deprenyl, to visualize astrogliosis in patients with neurological disorders. Clin Nucl Med **46**: e31-e33, 2021.
11. Mitamura K, Norikane T, Yamamoto Y, Miyake K, Nishiyama Y. Increased uptake of ^{18}F-THK5351 in glioblastoma but not in primary central nervous system lymphoma. Clin Nucl Med **46**: 772-773, 2021.

12. Kondo Y, Windrem MS, Zou L, et al. Human glial chimeric mice reveal astrocytic dependence of JC virus infection. J Clin Invest **124**: 5323-5336, 2014.